Journal of
Translational Regenerative Medicine

2026. Volume 1

Research Paper

In Vitro Osteogenesis and In Vivo Bone Formation Capacity of Macroporous Calcium Phosphate Cement

Saeed Hesaraki[1*], Davoud Sharifi[2], Javad Ashrafi-Helan[3], Nader Nezafati[1], Mostafa Shahrezaee[4*]

1. Department of Nanotechnology and Advanced Materials, Materials and Energy Research Center, Karaj, Iran.
2. Department of Clinical Sciences, Surgery and Radiology, Faculty of Veterinary Medicine, University of Tehran, Tehran, Iran.
3. Department of Veterinary Pathology, Faculty of Veterinary Medicine, University of Tabriz, Tabriz, Iran.
4. Department of Orthopedic Surgery, School of Medicine, AJA University of Medical Science, Tehran, Iran.

Use your device to scan and read the article online

Citation Hesaraki S, Sharifi D, Ashrafi-Helan J, Nezafati N, Shahrezaee M. In Vitro Osteogenesis and In Vivo Bone Formation Capacity of Macroporous Calcium Phosphate Cement. Journal of Translational Regenerative Medicine. 2025; 1:E1002. http://dx.doi.org/10.32598/JTRM.1.1002

http://dx.doi.org/10.32598/JTRM.1.1002

ABSTRACT

Background: Calcium phosphate cements (CPCs) are moldable microporous materials widely used for filling bone voids and defects. Introducing macro-porosity into the structure of these cements can enhance the biological functions and the rate of bone formation.

Methods: In this study, CPCs with different morphologies (non-porous and porous forms) were used as bone fillers. Different amounts of the porogen were used to obtain different macropore diameters. Bone marrow–derived mesenchymal stem cells (MSCs) were obtained from the tibial shaft of Wistar rats. MSC proliferation was assessed using the MTT assay. Real time PCR and analysis of gene expression for genes relevant to osteogenic differentiation of cells loaded on the samples were carried out. For in vivo evaluations, circular holes were created in the proximal epiphysis of the rabbit tibia bone. The holes were filled with non-porous and macroporous CPCs, and histomorphological evaluation was performed at 4 and 8 weeks after the operation.

Results: The results demonstrated that porous CPC was able to increase alkaline phosphatase activity and the expression of bone-related proteins (osteocalcin, osteopontin, and osteonectin) in MSCs cultured on the surfaces of cements. For in vivo evaluations, circular holes were created in the proximal epiphysis of the rabbit tibia bone. The holes were filled with non-porous and macroporous CPCs and histomorphologically evaluated at 4 and 8 weeks after the operation. The results revealed that, Wwhen the hole was filled with non-porous CPC, a layer of connective tissue with immature woven bone was formed at the surface of the implant without any resorption phenomenon. However, when the defect was filled with porous CPC (average pore diameter of 200 µm), the major part of the cement was resorbed and the resorbed cement was replaced by mature bone trabecula and unmineralized osteoid tissue.

Conclusion: The creation of macroporous cement could significantly improve the osteogenic ability and the active resorption rate of the cement, further associated with bone replacement by the host tissues.

Keywords: Bone remodeling, Calcium phosphate cement (CPCs), Osteogenesis, Porosity, In vivo

Article info:
Received: 06 Oct 2026
Accepted: 13 Dec 2025
Publish: 25 Jan 2026

*** Corresponding Authors:**
Saeed Hesaraki, Professor.
Address: *Department of Nanotechnology and Advanced Materials, Materials and Energy Research Center, Karaj, Iran.*
E-mail: *S-hesaraki@merc.ac.ir*

Mostafa Shahrezaee, Associate Professor.
Address: *Department of Orthopedic Surgery, School of Medicine, AJA University of Medical Science, Tehran, Iran.*
E-mail: *Moshahrezayee@yahoo.com*

Highlights

- CPCs are moldable microporous materials widely used for filling bone voids and defects.
- Porous CPC was able to increase alkaline phosphatase activity and the expression of bone-related proteins in MSCs.
- Creation of macroporous cement could significantly improve the osteogenic ability and the active resorption rate of the cement.

Plain Language Summary

Calcium phosphate cements (CPCs) are increasingly used for the repair of bone and periodontal defects. Introducing macroporosity into the structure of these cements can enhance the biological functions and the rate of bone formation. In this study, macroporosity was created in CPCs using a gas-foaming technique, and the in vitro osteogenesis, as well as the in vivo bone formation capacities, were investigated. The results demonstrated that porous CPC was able to increase alkaline phosphatase activity and the expression of bone-related proteins. Also, when the defect was filled with porous CPC, the major part of the cement was resorbed and the resorbed cement was replaced by mature bone trabecula and unmineralized osteoid tissue. In conclusion, creation of macroporous cements can significantly improve the osteogenic ability and the active resorption rate of the cement, further associated with bone replacement by the host tissues.

Introduction

Calcium phosphate cements (CPCs) are increasingly used as bone substitute materials in both dentistry and medicine for procedures, including the repair of bone and periodontal defects, the preservation or enhancement of the alveolar ridge, and as components in ear and eye implants, spinal fusion, and as adjuncts to uncoated implants [1-7] Recently, many studies have been performed on CPCs due to their injectability, high osteoconductivity, and gradual resorbability [8-12].

In addition to these advantageous characteristics, CPCs can act as delivery systems for cytokines, such as bone morphogenetic proteins (BMPs), insulin-like growth factors (IGFs), and transforming growth factors (TGFs), which stimulate recruited precursor cells from the host to develop into bone matrix [13]. However, a lack of macroporosity can limit the bone tissue growth into the cement implant [14].

The presence of large pores is essential for the growth of bone tissue in vivo because it allows osteoblasts and mesenchymal cells to migrate and proliferate, and also allows matrix to be deposited in the open spaces [15].

Although macroporosity strongly influences osteogenic outcomes, the interconnecting pathways and the size of the macropores are also important factors [16]. Previously, macroporous CPCs have been produced using various methods based on different mechanisms, such as leaching out crystals (e.g. mannitol, sucrose, and sodium carbonate) or resorbable fibers, melting mixtures of frozen solution particles, oil dispersion, gas-generating processes (like O_2 from H_2O_2 decomposition or CO_2 formed by acid–base reactions), and trapping air bubbles [17-25].

Recently, the formation and evaluation of macroporous CPC using an effervescent additive was reported [26, 27].

The present work deals with the osteogenic capacity and histomorphological study of the healing process of porous CPC-substituted circular defects in the proximal epiphysis of the rabbit tibia.

Materials and Methods

Preparation of calcium phosphate cements

In this study, CPCs with different morphologies (non-porous and porous forms) were used as bone fillers. The cements were prepared in accordance with our previous works [26, 27]. In brief, a mixture of tetracalcium phosphate (TTCP) and dicalcium phosphate anhydrate (DCPA) at molar ratio of 1:1 was used as the powder phase. A solution of 6% disodium hydrogen phosphate

and 0.5% sodium alginate was used as the liquid phase of the cement.

To create macroporous CPCs, an effervescent agent (a mixture of citric acid and $NaHCO_3$) was introduced into the cement composition. Different amounts of the porogen were used to obtain different macropore diameters. The cements with pore diameters of 100 and 200 µm were named AC-1 and AC-2, respectively.

Cell studies

Cell culture

Bone marrow–derived mesenchymal stem cells (MSCs) were obtained from the tibial shaft of Wistar rats. The cells were cultured in Dulbecco's modified eagle medium (DMEM; Gibco-BRL, Life Technologies, Grand Island, NY) supplemented with 15% fetal bovine serum (FBS) and 100 µg/mL penicillin–streptomycin. The bone marrow suspensions were seeded in polystyrene 6-well plates. After four days, non-adherent cells were removed through phosphate-buffered saline (PBS) washes and medium replacement. Adherent cells were expanded as monolayers at 37 ˚C in a 5% CO_2 environment, with medium refreshed every three days. Once confluent, the cells were detached using 0.05% trypsin/EDTA and transferred to new 6-well plates at a density of 5×10^4 cells per dish. This process was repeated until a sufficient number of cells was obtained.

Cell seeding on samples

In all cases, samples with a diameter of 1 cm were loaded with 10^4 cells obtained from the third subculture of MSCs. Cell-loaded samples were incubated in 15% FBS-supplemented DMEM for 1, 3, 7 and 14 days. The dish culture was used as the control group.

MTT assay

MSC proliferation was assessed using the MTT (3-{4,5-dimethylthiazol-2-yl}-2,5-diphenyl-2H-tetrazolium bromide) assay. After removing the culture medium, 2 mL of an MTT/cell culture medium solution (1:5) was added to each well. The plates were then incubated for 2 hours at 37 ˚C in a humidified atmosphere with 5% CO_2. Afterward, the medium was discarded, and the resulting formazan crystals were dissolved in DMSO. The optical density was measured at 540 nm using a microplate spectrophotometer. Analyses were conducted on days 1, 3, 7, and 14 following cell seeding on the samples.

Alkaline phosphatase (ALP) activity assay

ALP activity of the cell–disc constructs was assessed on days 1, 3, 7, and 14 following seeding. After washing, the samples were lysed and the resulting mixtures were clarified. Portions of the supernatant were combined with a p-nitrophenol phosphate substrate and an alkaline buffer, and allowed to react before being stopped. Absorbance was recorded at 405 nm, and a concurrent standard curve of known p-nitrophenol concentrations enabled quantification. ALP activity, expressed as nanomoles of substrate converted per minute, was normalized to the total protein content measured with a colorimetric protein assay.

Cell morphology on cements

The cell morphology was evaluated on the samples cultured for 14 days. After the culture medium was removed, MSC-seeded samples were briefly rinsed with PBS and subsequently fixed using a glutaraldehyde solution. Following a short fixation period, they were washed again and stored in PBS at 4 ˚C. A secondary fixation was then carried out using osmium tetroxide. The samples were gradually dehydrated through a series of increasing ethanol concentrations and allowed to dry completely. Once dried, they were mounted, coated with a thin layer of gold, and examined using scanning electron microscopy (SEM).

Osteogenesis capacity by reverse transcription polymerase chain reaction (RT-PCR) and real-time PCR

RT-PCR and real-time analysis of gene expression for genes relevant to osteogenic differentiation of cells loaded on the samples were carried out. Briefly, after 14 days of culture, total RNA was collected from loaded cells using RNXPlusTM solution (CinnaGen Inc., Tehran, Iran). The standard reverse transcription reaction was performed using the RevertAid™ H Minus First Strand cDNA Synthesis Kit (Fermentas) according to the manufacturer's instructions. Subsequent PCR was as follows: 2.5 µL cDNA, 1x PCR buffer (AMS), 200 µM dNTPs, 0.5 µM of each primer pair, and 1 unit of Taq DNA polymerase (Fermentas). The mentioned primers were utilized to detect osteogenic differentiation. Each PCR was done in triplicate. The products were assessed on a 2% agarose gel and visualized by ethidium bromide staining.

Table 1. Distribution of animal groups and porosity information of cements used for filling bone defects

Evaluation Time	Implant Type	Group Name	Macroporosity (%)	Macropore Size (µm)	Total Porosity (%)
Four weeks (I)	No implant	Ia	-	-	-
	Non-porous CPC	Ib	-	-	55
	Porous AC-1	Ic	16	100	61
	Porous AC-2	Id	23	200	66
Eight weeks (II)	No implant	IIa	-	-	-
	Non-porous CPC	IIb	-	-	55
	Porous AC-1	IIc	16	100	61
	Porous AC-2	IId	23	200	66

Real-time PCR analysis was performed following the established methods. In brief, the procedure included RNA extraction, quantitative assessment of RNA quality and concentration, DNase I treatment to remove genomic DNA contamination, cDNA synthesis, primer design, and determination of relative gene expression levels using real-time PCR. All PCR assays were conducted after 28 days under the specified conditions, with five replicates for each sample.

In vivo evaluations

Implantation

The experiment was conducted on 40 adult New Zealand white rabbits, which were divided into four groups of 10 rabbits each (a, b c, and d). Then, each group was subsequently divided into two subgroups of five rabbits each, namely I (4 weeks) and II (8 weeks) duration (Table 1).

Then, the rabbits were shaved and disinfected in the areas over the right radii or tibias after general anesthesia with a mixture of 10% ketamine hydrochloride and xylazine hydrochloride (1 mL/kg). A hole measuring 5×5 mm in diameter and depth was made in the inner aspect of the right proximal epiphysis of the tibia in each rabbit using a sterile 701 fissure bur.

In subgroups Ia and IIa, which served as control groups, the defects were left empty for healing observation and comparison with the healing aspects of the other sub-

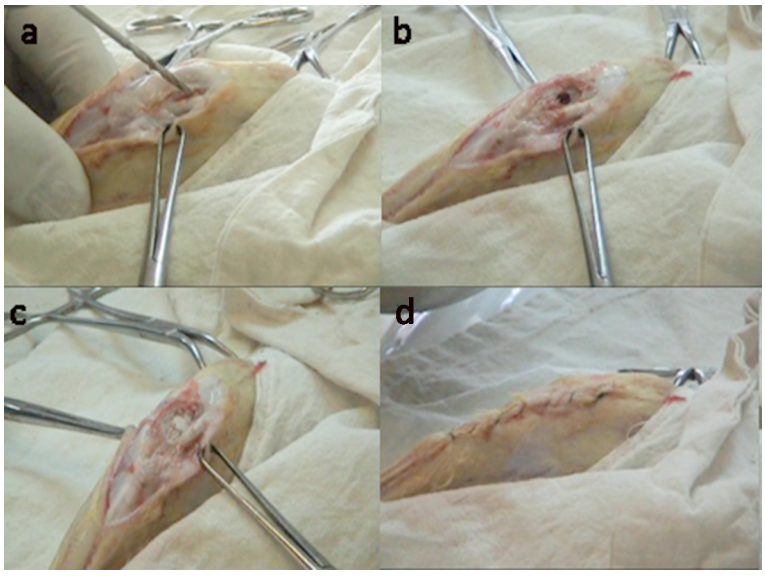

Figure 1. Creation of a defect in the inner aspect of the right proximal epiphysis of the rabbit tibia

a) Drilling, (b) Hole creation, (C) Hole filled with cement, (d) Suturing to close the wound

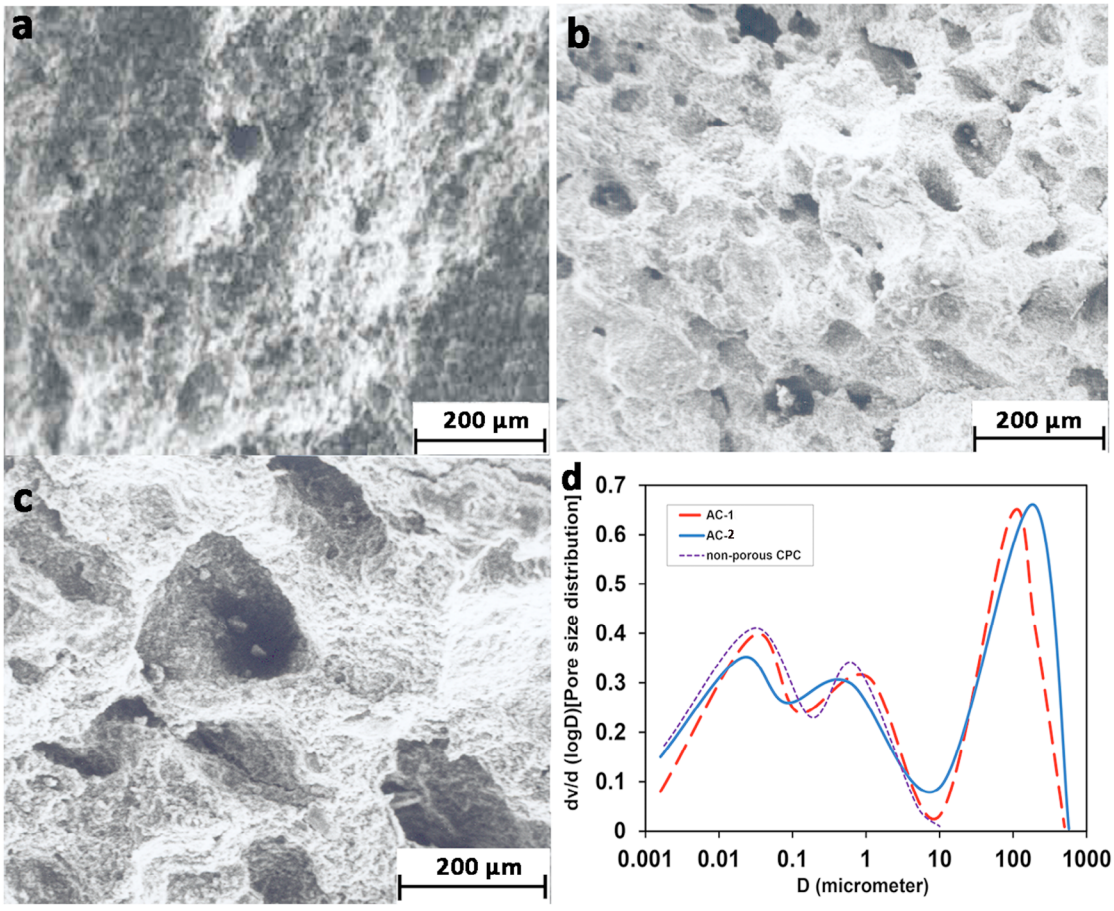

Figure 2. The scanning electron micrographs of CPCs

a) Non-porous CPC, b) Porous AC-1, c) AC-2, d) Pore size distribution curves of the cements

groups. The non-porous CPC was used to fill the bone defect in subgroups Ib and IIb, while the defects were filled with macroporous CPCs with 61% porosity and an average pore diameter of 90 µm (AC-1) in subgroups Ic and IIc, and 66% porosity with an average pore diameter of 190 µm (AC-2) in subgroups Id and IId (Table 1). The periosteum, muscle, and skin were reapproximated and sutured with 3-0 nylon. Figure 1 shows the various steps of hole creation in the rabbit tibia bone. In the postoperative period, the rabbits were placed in individual cages and received water and laboratory rabbit chow ad libitum. The rabbits were sacrificed with intracardiac injection of saturated thiopental sodium (10%) at 4 and 8 weeks postoperatively. The tibia was cut from each epiphysis of the implantation site, and the samples were sent for histomorphological analysis.

Histopathological analysis

Bone segments fixed in 10% neutral buffered formaldehyde solution were decalcified, embedded in paraffin, and sectioned at 6 µm. The sections were obtained parallel (serial sections) and transverse to the long axis of the cement implants. Each section of the bone segments was stained using the Hematoxylin and Eosin (H&E) method to study the quality of new bone, the condition of cement resorption, and the presence of soft tissue and inflammatory cells [28-31].

Statistical analysis

All data were analyzed using Microsoft Excel 2021. A minimum of four specimens from each composition were tested, and the results are reported as Mean±SD. Statistical significance among mean values was assessed by analysis of variance (ANOVA), followed by Tukey's post hoc test (SPSS software, version 10.0, Chicago, IL, USA), with differences considered significant at $P<0.05$.

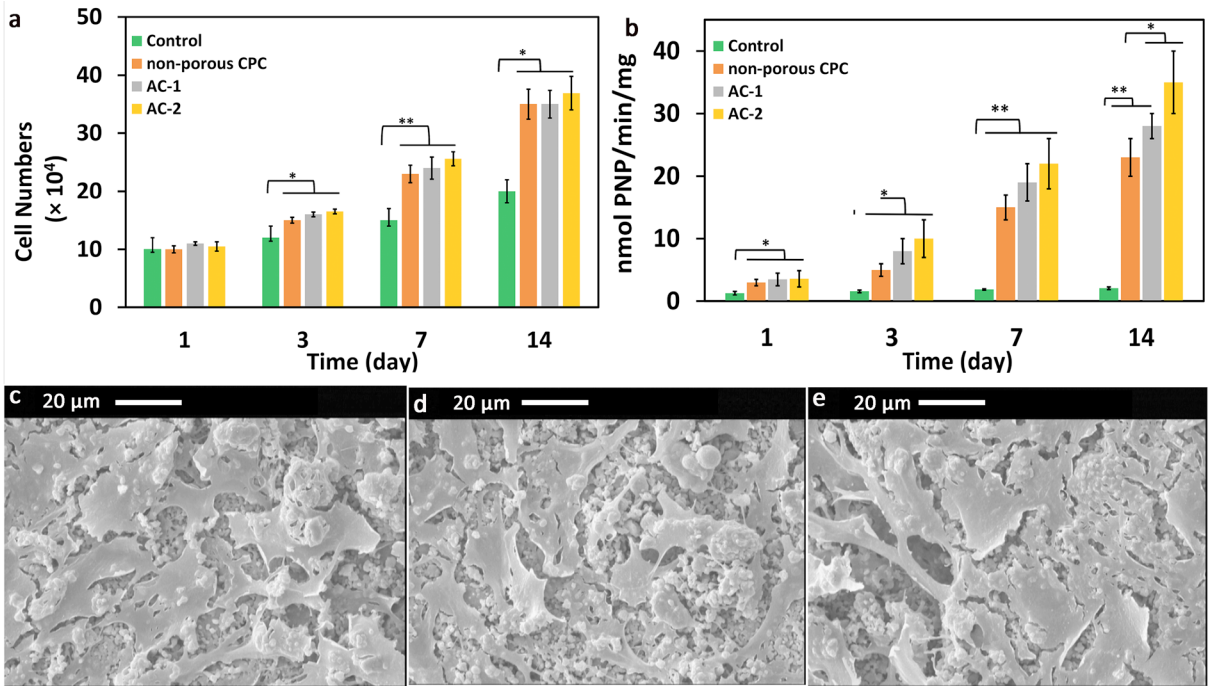

Figure 3. The proliferation (a) and ALP activity (b) of CPCs on various cements, compared to the control group

*P<0.005, **P<0.001).

Note: The morphology of the cells on various cements is also shown: Non-porous cement (c), AC-1 (d), and AC-2 (e).

Results

Morphological aspects of the cements

Figure 2 shows the SEM micrographs and pore size distribution of cements. In the non-porous cement (Figure 2a), a microporous structure with a rough feature is observed. In macro-porous cements (Figures 2b and 2c), large macropores are clearly observed. The size of the pores is larger in cement AC-2 (Figure 2c). Figure 2d shows the pore size distribution of the cements. In the non-porous cement, a bimodal size distribution is observed, with pore sizes concentrated at 0.1 and 1 µm. The size of the macropores is focused at 100 and 200 µm for AC-1 and AC-2, respectively.

Cell proliferation, ALP activity, and osteogenesis

To evaluate the proliferation capacity of the samples, the direct culture method was employed, and the MTT assay was performed on days 1, 3, 7, and 14. As shown in Figure 3a, in both the control group and the cement samples (non-porous cement, AC1, and AC2), the number of cells increased over time, and this increase continued until day 14. The number of cells on cements was much higher than that of the control group; however, no significant difference was observed between the cements in terms of cell number and growth rate.

The results of ALP activity measurement for the control group and cement samples are presented in Figure 3b. Accordingly, the enzyme activity in the cement samples was significantly higher than that of the control samples on days 1, 3, 7, and 14, and showed an increasing trend during this period (P<0.05). Except for day 14, no significant differences were observed among the cement samples; however, the average ALP value of the AC-2 was higher than that of the others. On day 14, the AC-2 sample exhibited the highest level of ALP activity, which was significantly different from the other samples. The increase in ALP activity indicated the osteogenic differentiation of stem cells and the onset of their osteoblastic activity. The elevated ALP activity observed in the cement samples compared to the controls highlights the bioactivity and osteoinductive potential of the tested materials. ALP is a well-established early marker of osteogenic differentiation, and its upregulation in the AC-2 sample, particularly on day 14, indicates enhanced osteoblastic activity and mineralization capacity. These findings are consistent with previous reports demonstrating that calcium-based biomaterials can promote osteogenesis by providing a favorable microenvironment for stem cell differentiation.

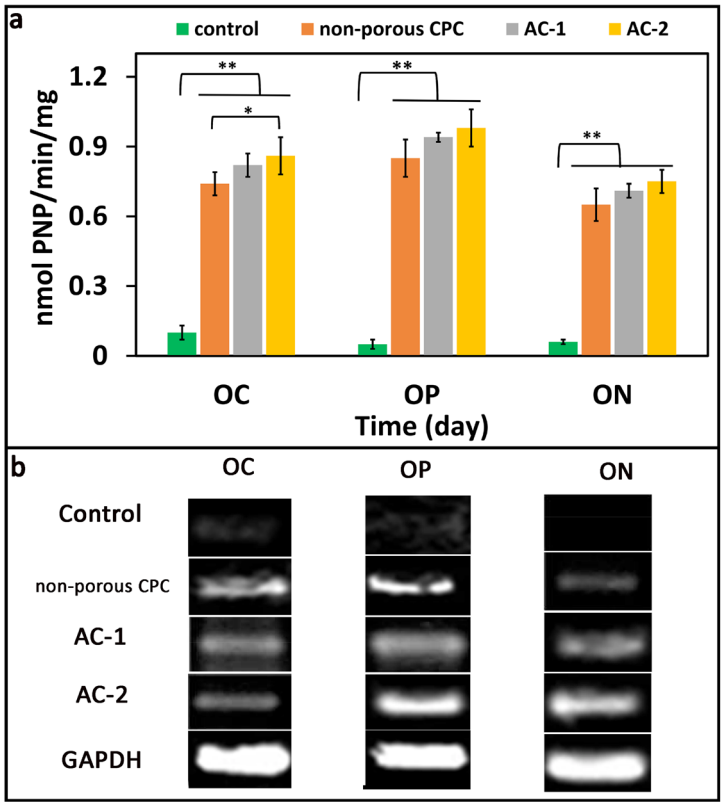

Figure 4. The expression of osteocalcin (OC), osteopontin (OP), and osteonectin (ON) proteins by MSCs on the surfaces of calcium phosphate cements

*P<0.005, **P<0.001.

Note: Data were obtained by real-time PCR (a) and RT-PCR (b).

The superior performance of AC-2 suggests that its physicochemical composition may further stimulate osteoblastic responses, making it a promising candidate for bone regeneration applications.

Figures 3c, 3d and 3e illustrates the morphology of cells cultured on the surface of the cement samples. As shown, the cells continued to proliferate over time and completely covered the sample surface by day 14 post-seeding. Stem cells adhered well to the cement samples and exhibited consistent proliferation. In all cement samples, the cells displayed lamellipodia and filopodia morphology, and the formation of nodules on the cell surface was clearly observed. The observed morphology reflects the favorable surface characteristics of the samples in terms of their physicochemical properties and lack of cytotoxicity.

The progressive proliferation and complete surface coverage observed by day 14 confirm that the cement samples provide a biocompatible substrate supportive of cell adhesion and growth. The presence of lamellipodia and filopodia suggests active cell–substrate interactions, which are critical for cytoskeletal organization and subsequent osteogenic differentiation. Moreover, the appearance of nodular structures indicates the initiation of extracellular matrix mineralization, an essential step in bone tissue formation. These findings suggest that the cement surfaces (specifically AC-2, Figure 3e) not only support cell viability but also create a microenvironment conducive to osteogenic activity, thereby underscoring their potential application in bone regeneration therapies.

Real-time PCR (Figure 4a) and RT-PCR (Figure 4b) using primers targeting osteopontin, osteocalcin, and osteonectin assessed the expression of osteogenic differentiation–related genes in cells grown on the various cement samples for 14 days. *GAPDH* served as the internal reference gene. As shown in Figure 4, all the aforementioned genes were expressed in cells cultured on the various cement samples, whereas cells cultured on the control samples did not exhibit the expression of these genes. The observed expression of osteopontin, osteocalcin, and osteonectin genes in cells cultured on cement samples strongly supports the osteoinductive potential of

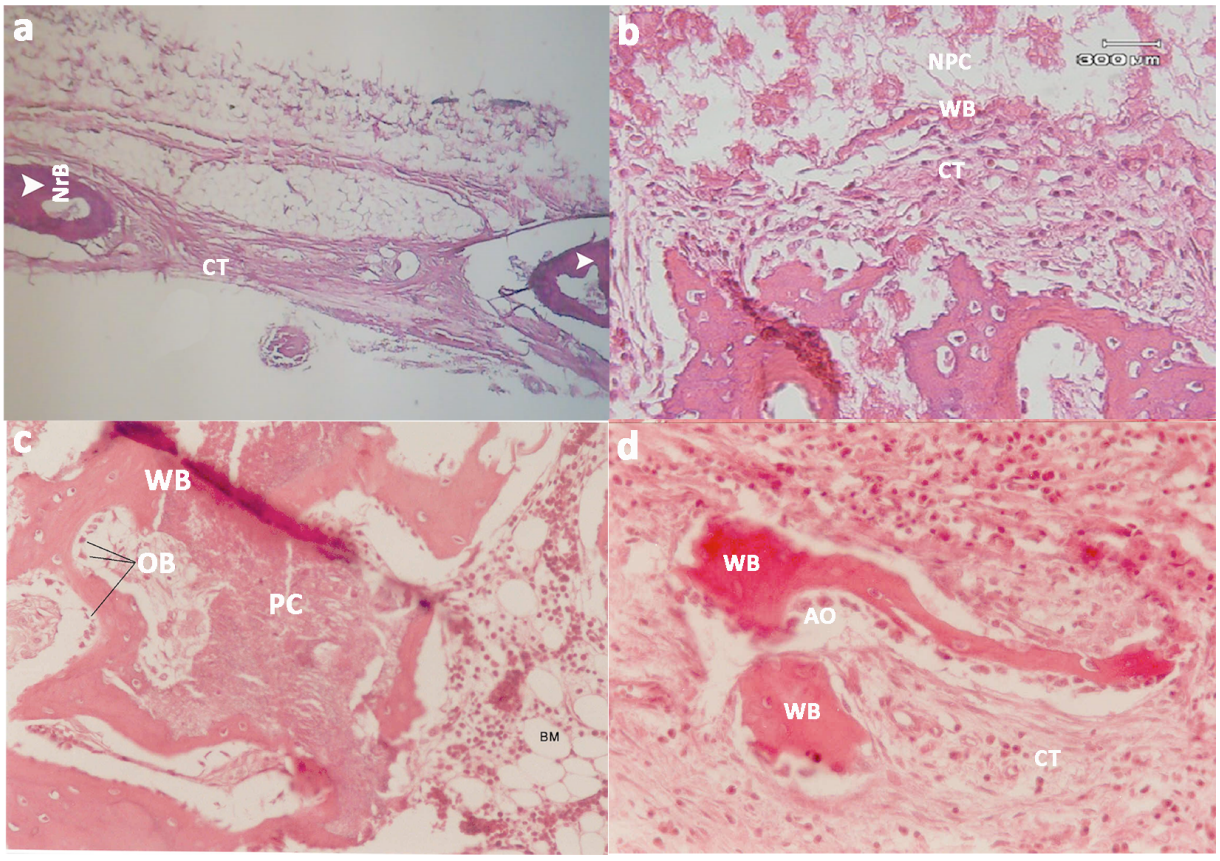

Figure 5. The results of histopathology as optical micrographs of bone defects after 4 weeks of implantation

Note: a) In subgroup Ia, the defect was filled with soft CT. No bone formation was observed. The normal bone (NrB) is seen at the tip of the arrow. No significant inflammatory reaction was found (staining with H&E ×70). b) In subgroup Ib, a slight amount of the non-porous cement (NPC) was resorbed and covered by CT containing newly formed bone. A thin layer of immature woven bone (WB) surrounded the implant surfaces (H&E ×400). C) In subgroup Ic, the cement (PC) was resorbed and covered by CT containing newly formed bone. A thin layer of immature woven bone (WB) surrounded the implant surface. Active osteoblasts (OB) were also observed (staining with H&E ×150). d) In subgroup Id, the porous cement was degraded, and bone formation occurred. Newly formed bone trabeculae (WB) are presented in the picture. These trabeculae are lined by active osteoblasts (AO). The gap between the trabeculae has been filled with CT containing fibroblasts, differentiating osteoblasts, and mononuclear inflammatory cells (staining with H&E ×210).

these materials. These genes are well-established markers of osteogenic differentiation: osteopontin is involved in cell adhesion and early mineralization, osteocalcin is associated with late-stage osteoblast maturation, and osteonectin plays a role in matrix remodeling and mineral deposition. The absence of expression in the control group highlights the critical role of the cement substrates in directing stem cells toward an osteogenic lineage. These findings suggest that the tested cements not only provide a biocompatible surface but also actively promote molecular pathways required for bone formation, further validating their potential utility in regenerative medicine and bone tissue engineering.

In vivo outcomes

Macroscopic observation

After the materials were implanted in the rabbit defects, all the wounds healed gradually and the rabbits were active with no post-surgery complications. No operative or postoperative complications were encountered. All rabbits tolerated surgery well and survived until the final experimental time. No wound openings or infections were observed. The macroscopic evaluation revealed the maintenance of the correct position of the sample in the tibial site.

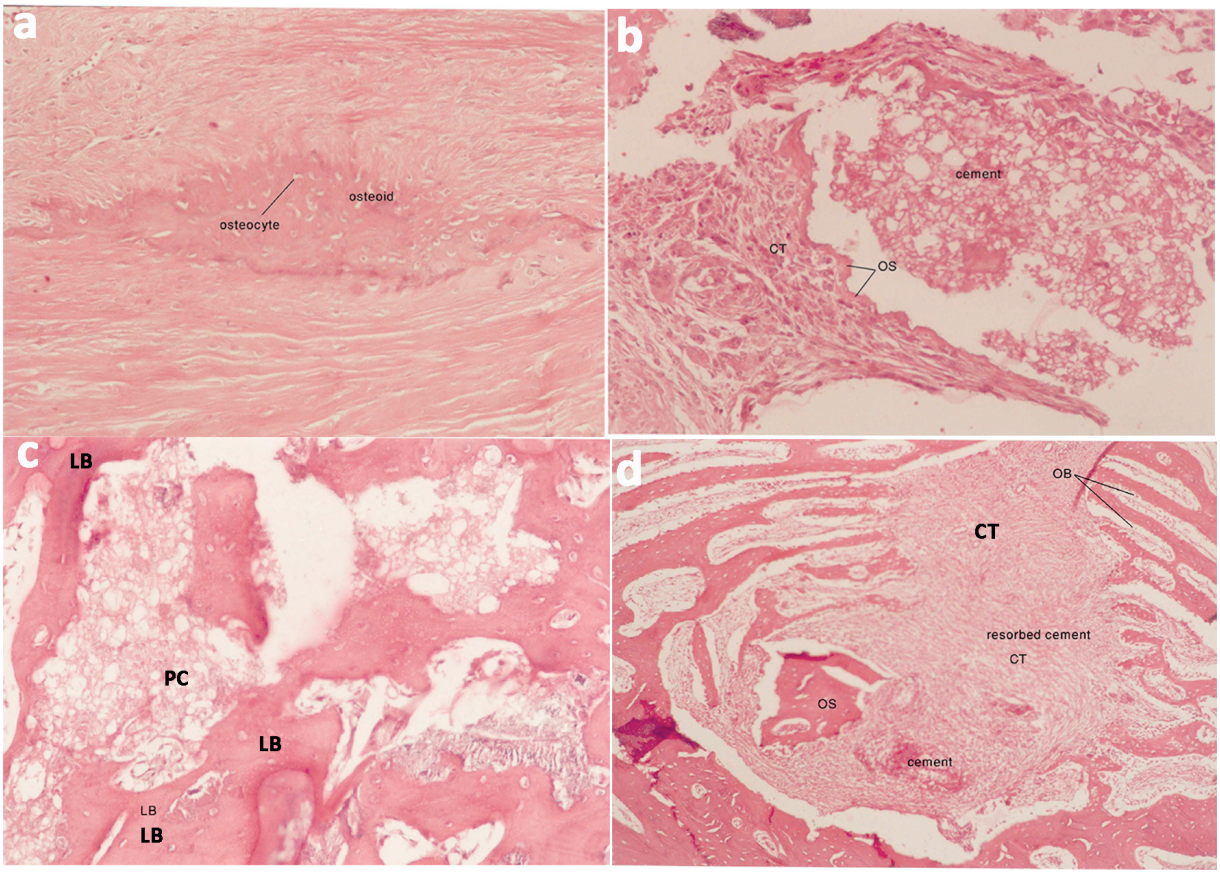

Figure 6. The results of histopathology as optical micrographs of bone defects after 4 weeks of implantation

Note: a) In subgroup IIa, the holes were completely filled with dense CT containing parallel collagen bundles, unmineralized osteoid tissue, and immature bone trabecular structures with low maturation and many remodeling marks (staining with H&E ×192). b) In subgroup IIb, the non-porous implants were surrounded by CT. However, a thin layer of immature woven bone covered the implant surface. The integrity of the non-porous implants was relatively maintained, and a small amount of cement was resorbed. In this subgroup, there were no signs of extensive cement degradation, and the gap between the cement implant and surrounding bone was filled with CT containing newly formed bone that completely covered the implants (staining with H&E ×240). C) In subgroup IIc, a few grains of the cement (PC) detached from the implant (H&E ×165). d) In subgroup IId, newly formed immature woven bone (WB) trabeculae and relatively mature lamellar bone trabeculae (LB) are present. These trabeculae are lined by active osteoblasts (OB). Between these trabeculae and the porous cement remnants, CT containing fibroblasts, differentiating osteoblasts, and mononuclear inflammatory cells is seen (staining with H&E ×46).

Qualitative histological observation

Figures 5 and 6 represent the histopathological observation of various groups after 4 and 8 weeks of implantation, respectively. The histological inspection of sections of all subgroups revealed no evidence of severe infection, inflammation, or necrosis of the tissue surrounding the implant.

Control group (group a): The histopathological examinations of control groups revealed that the holes in subgroup Ia (Figure 5a) were entirely filled with connective tissue (CT) containing thin and relatively parallel collagen fibers undergoing mineralization. The unmineralized bone matrix (osteoid tissue), centers of ossification, immature bone trabeculae fragments, mesenchymal cells, numerous dilated capillaries, and a few inflammatory cells were noticed. Ossification had begun at the edges of the defect. In subgroup IIa (Figure 6a), the holes were completely filled with dense CT containing parallel collagen bundles, unmineralized osteoid tissue and immature bone trabecular structures with low maturation and many remodeling marks.

Non-porous CPC group (group b): In treatment group b, where the holes were filled with non-porous CPC implant (subgroup Ib), light microscopy revealed that the non-porous implants were covered by layers of collagen fibers. On the cement surface, a thin layer of early woven bone of poor quality and a layer of mononuclear and multinucleated phagocytic cells were observed (Figure 5b).

At eight weeks after implantation (Figure 6b), the non-porous implants were surrounded by CT. However, a thin layer of immature woven bone covered the implant surface. The integrity of the non-porous implants was relatively maintained, and a small portion of the cement was resorbed.

In this subgroup, there were no signs of extensive cement degradation, and the gap between the cement implant and surrounding bone was filled with CT containing newly formed bone that completely covered the implants. Bone formation, which began at the edges of the defect and originated from the defect wall, was also noticed. In these regions, the bone trabeculae were oriented from the cortical zone. These trabeculae were immature woven bone that was covered by active osteoblasts and undergoing maturation. A few particles of the cement were detached from the implants and initiated a focal foreign body reaction in the soft tissues surrounding the materials, along with thin, newly formed bone fragments.

Macroporous AC-1 group (group c): In the treatment group where holes were filled by macroporous CPC implants with 61% porosity and an average pore diameter of 100 µm (AC-1), the implantation zone was occupied by a porous material mass with pores within the matrix that had been partially removed from the sections by a microtome blade (Figure 5c). A slight portion of the porous cement was resorbed and replaced with a thin layer of newly formed immature woven bone trabeculae. The outer surface of the porous sample was totally lined with CT that frequently filled the gap between the implant surface and the defect wall. This CT contained relatively parallel collagen fibers, numerous blood vessels, active fibroblasts, and many fibroblast-like cells, along with differentiating osteoblasts that formed an osteoid matrix and bone trabecular fragments. A layer of macrophages and multinucleated giant cells surrounding the cement surface was observed. Bone formation ranged from limited to more extensive degrees. When limited bone formation occurred, only some osteoid on top of a layer of osteoblasts inside the porosity was observed. In cases of extensive bone formation, the mineralization and maturation processes of the osteoid had begun. There was no evidence of callus formation between the implant surface and the wall of the drill holes. There was, however, evidence of bony trabeculae that originated from the cortical zone of the drill wall and inserted perpendicularly into the implant surface. These trabeculae were surrounded by an osteoid layer lined with active osteoblasts and exhibited remodeling marks.

Subgroup IIc (Figure 6c), in comparison to subgroup Ic (Figure 5c), shows more cement resorption and replacement by immature woven bone trabeculae. The width, length, and bone maturation of newly formed bone trabeculae were more prominent at 8 weeks than at 4 weeks, and some of them showed lamella-like structures. In this subgroup, the trabeculae originated from the drill wall, linked to those trabeculae formed within the CT and surrounded the cement remnants. In this subgroup (IIc, Figure 6c), the cement material remnants exhibited a matrix with irregular porosity, and dark, small granules appeared to be foreign body contamination of the cement. Around the cement, macrophages and giant cells were evident and resorption marks at the implant surface and mineralizing bone trabeculae ingrown into the cement surface, were apparent. Similar granules were found within macrophages and giant cells. A few grains of the material had become detached from the cement and were found free in the reactive CT in the bone marrow cavity and surrounding soft tissues. In some sites, the natural bone marrow cavities in undisrupted bones were completely filled with the cement.

Macroporous AC-2 Group (group d): In the treatment group where holes were filled with the macroporous implant of AC-2, after 4 weeks (Figure 5d), the slit between the implant surface and the drill wall was filled with mature CT that was broadly replaced by immature bone trabeculae, completely bridging the gap, and a solid mineral core was present. The bone trabeculae structure was immature, with many remodeling marks. In certain regions, remnants of the porous cement were observed between newly formed bone trabeculae or within the CT, where differentiated osteoblasts had produced osteoid matrix and bone trabecula fragments. Macrophages and giant cells also phagocytosed many particles detached from the cement. Bone formation had begun in the cement pores and at the outer surface of the cement.

In subgroup IId (Figure 6d), the majority of the cement was resorbed, leaving only some fragments and small scattered remnants. Around the cement particles, reactive CT containing inflammatory cells, especially macrophages and giant cells, was clearly observed, and the remnant porous cement particles were still subjected to degradation by phagocytic cells. Abundant small dark granules, which seemed to be foreign body contamination, were present in the cement remnants and were phagocytosed by macrophages and giant cells.

The resorbed cement was substituted by bone trabecular structures and unmineralized osteoid tissue. The bony trabeculae were relatively mature, showing lamella-like

structures and bone marrow space formation. The width, length, and quality of the trabeculae in subgroup IId (Figure 6d) were more than those in subgroup Id (Figure 5d). In this region, a mesenchymal soft tissue was located between trabeculae. In the newly formed bone trabeculae, evidence of the remodeling phase was clear, and the trabeculae could still be recognized from the drill wall. However, in this subgroup (subgroup IId), the degree of maturation of newly formed bone was relatively similar to that of the natural bone at undisturbed sites. Bone marrow cavities were focally filled with porous cement fragments. These foci, embedded with the dense tissue, contained reactive CT, a foreign body reaction, and thin bone trabeculae.

Discussion

In this study, the porous cement was well tolerated and induced a mild foreign body reaction, which did not impair its replacement by newly formed bone within a few weeks. In this experiment, the cement did not seem to induce any necrosis as no dead tissue zone was visible 4 and 8 weeks after implantation. Histological findings showed better integration in the porous experimental groups than in the non-porous and control subgroups. Bone maturation was marked by the arrangement of collagen fibers, activated fibroblasts, and the formation of lamella-like structures. The present study revealed that the tissue responses to the porous implants at 4 and 8 weeks after implantation were completely different from those observed with non-porous cement and control subgroups. In the non-porous cement implant, the cement surface acted as a scaffold for bone guidance. In contrast, the porous cements evoked a completely different bone response. The porous cements, especially with larger pores (AC-2), stimulated bone formation and were rapidly integrated into bone tissue. In the current study, the porous cement was almost completely surrounded by immature bone. Histopathological evidence showed that bone formation appeared to begin in the center of the pores and at the outer surface of the cement due to osteoconduction. However, bone formation that occurred inside the implant pores, especially after 4 weeks, seemed to result from osteoinduction. At 8 weeks after implantation, there was a significant increase in the amount of bone trabeculae in the sites implanted with the porous cements compared to the non-porous cement and control sites.

The degradation rate and the growth of bone-forming trabeculae within the resorbed materials of AC-1 and AC-2 were relatively higher than that of non-porous cement. The initial attachment and subsequent proliferation of osteogenic cells, as well as their ability for bone formation are the most important factors that affect the success of a bone substitute [32]. Osteoblast differentiation occurs at the surface of the porous cement and within the pores, leading to the presence of an osteoblast line that synthesizes an osteoid matrix and subsequently forms immature bone. When the material surface is coated by immature bone trabeculae, the bone spicules extend throughout the entire pore volume. It appears that the high surface area of the material, combined with the high solubility of the matrix, induces a favorable microenvironment around the cement. The degradation rate of the material is compatible with the ingrowth of the bone tissue within the degraded cement. In the porous CPCs, both the active and passive resorption rate and bone tissue replacement, were increased due to the enhancement of specific surface area and tissue growth into the material's porosity. Another objective of the present study was to determine the role of macropore size in the rates of implant resorption and bone formation.

There are several studies [33-37] that attempt to determine an optimum macropore size. However, there is no obvious optimum macropore size for implant resorption or bone formation because many parameters affect it. These include, for example, animal species, defect size, implant resorption, implant chemistry, implant topography, and pore fraction. Although tissue response to the cement implant was less affected by the macropore size, in the present study, AC-2 with a macropore size of 200 µm was resorbed faster than AC-1 with a macropore size of 100 µm.

Conclusion

Macroporous CPCs were assessed in terms of osteogenesis and bone formation ability. MSCs proliferated on the surfaces of the cements regardless of macroporosity. Macroporosity increased the differentiation of the cells and improved the expression of bone-related proteins. Moreover, the creation of macropores can significantly improve the degradation and the active resorption rate of the CPC, which is associated with almost complete bone replacement. The macroporous CPC is biocompatible and characterized by the fast deposition of new bone on the cement surface. In this study, the duration of the experiment was slightly too short to investigate the complete resorption of the porous cement. Further attention is also needed to evaluate the osteoinductive behavior of the porous cement.

Ethical Considerations

Compliance with ethical guidelines

There were no ethical considerations to be considered in this research.

Funding

This research did not receive any grant from funding agencies in the public, commercial, or non-profit sectors.

Authors' contributions

All authors contributed equally to the conception and design of the study, data collection and analysis, interception of the results and drafting of the manuscript. Each author approved the final version of the manuscript for submission.

Conflict of interest

The authors declared no conflict of interest.

References

[1] Costantino PD, Friedman CD, Lane A. Synthetic biomaterials in facial plastic and reconstructive surgery. Facial Plastic Surgery. 1993; 9(1):1-15. [DOI:10.1055/s-2008-1064591] [PMID]

[2] Wolfe SA. Correction of a lower eyelid deformity caused by multiple extrusions of alloplastic-orbital floor implants. Plastic and Reconstructive Surgery. 1981; 68(3):429-32. [DOI:10.1097/00006534-198100000-00037]

[3] Wang J, Chen W, Li Y, Fan S, Weng J, Zhang X. Biological evaluation of biphasic calcium phosphate ceramic vertebral laminae. Biomaterials. 1998; 19(15):1387-1392. [DOI:10.1016/S0142-9612(98)00014-3] [PMID]

[4] Kent JN, Block MS, Finger IM, Guerra L, Larsen H, Misiek DJ. Biointegrated hydroxylapatite-coated dental implants: 5-year clinical observations. Journal of the American Dental Association. 1990; 121(1):138-44. [DOI:10.14219/jada.archive.1990.0138] [PMID]

[5] Hupp JR, Mckenna S. Use of porous hydroxylapatite blocks for augmentation of atrophic mandibles. Journal of Oral and Maxillofacial Surgery. 1988; 46(7):538-45. [DOI:10.1016/0278-2391(88)90143-7] [PMID]

[6] Friedman CD, Costantino PD, Jones K, Chow LC, Pelzer HJ, Sisson GA. hydroxyapatite cement: II, Obliteration and reconstruction of the cat frontal sinus. Archives of Otolaryngology--Head & Neck Surgery. 1991; 117(4):385-389. [DOI:10.1001/archotol.1991.01870160039005] [PMID]

[7] Hong YC, Wang JT, Hong CY, Brown WE, Chow LC. The periapical tissue reaction to a calcium phosphate cement in the teeth of monkeys. Journal of Biomedical Materials Research 1991; 25(4):485-98. [DOI:10.1002/jbm.820250406] [PMID]

[8] Yoshimine Y, Sumi M, Isobe R, Anan H, Maeda K. In vitro interaction between tetracalcium phosphate-based cement and calvarial osteogenic cells. Biomaterials. 1996; 17(23):2241-3. [DOI:10.1016/0142-9612(96)00045-2] [PMID]

[9] Frayssinet P, Gineste L, Conte P, Fages J, Rouquet N. Short-term implantation effects of a DCPD-based calcium phosphate cement. Biomaterials. 1998; 19(11-12):971-7. [DOI:10.1016/S0142-9612(97)00163-4] [PMID]

[10] Chow LC. Calcium phosphate cements: Chemistry, properties, and applications. MRS Online Proceedings Library. 2000; 599:27-37. [DOI:10.1557/PROC-599-27]

[11] Costantino PD, Friedman CD, Jones K, Chow LC, Sisson GA. Experimental hydroxyapatite cement cranioplasty. Plastic and Reconstructive Surgery. 1992; 90(2):174-85. [DOI:10.1097/00006534-199290020-00003]

[12] Friedman CD, Costantino PD, Takagi S, Chow LC. BoneSource™ hydroxyapatite cement: a novel biomaterial for craniofacial skeletal tissue engineering and reconstruction. Journal of Biomedical Materials Research. 1998; 43(4):428-32. [DOI:10.1002/(SICI)1097-4636(199824)43:43.0.CO;2-0]

[13] Ginebra MP, Traykova T, Planell JA. Calcium phosphate cements as bone drug delivery systems: A review. Journal of Controlled Release. 2006; 113(2):102-10. [DOI:10.1016/j.jconrel.2006.04.007] [PMID]

[14] Mastrogiacomo M, Scaglione S, Martinetti R, Dolcini L, Beltrame F, Cancedda R, et al. Role of scaffold internal structure on in vivo bone formation in macroporous calcium phosphate bioceramics. Biomaterials. 2006; 27(17):3230-7. [DOI:10.1016/j.biomaterials.2006.01.031] [PMID]

[15] Kuboki Y, Takita H, Kobayashi D, Tsuruga E, Inoue M, Murata M. BMP-induced osteogenesis on the surface of hydroxyapatite with geometrically feasible and nonfeasible structures: Topology of osteogenesis. Journal of Biomedical Materials Research. 1998; 39(2):190-9. [DOI:10.1002/(SICI)1097-4636(199802)39:23.0.CO;2-K]

[16] Barou O, Mekraldi S, Vico L, Boivin G, Alexandre C, Lafage-Proust MH. Relationships between trabecular bone remodeling and bone vascularization: A quantitative study. Bone. 2002; 30(4):604-12. [DOI:10.1016/S8756-3282(02)00677-4] [PMID]

[17] Takagi S, Chow LC. Formation of macropores in calcium phosphate cement implants. Journal of Materials Science: Materials in Medicine. 2001; 12(2):135-9. [DOI:10.1023/A:1008917910468]

[18] Yoshikawa T, Suwa Y, Ohgushi H, Tamai S, Ichijima K. Self setting hydroxyapatite cement as a carrier for bone-forming cells. Bio Med Mater Eng. 1996; 6(5):345-51. [DOI:10.3233/BME-1996-6504]

[19] Markovic M, Takagi S, Chow LC. Formation of macropores in calcium phosphate cements through the use of mannitol crystals. Paper presented at: Proceedings of the 13th International Symposium on Ceramics in Medicine; Bioceramics 13. 2000 November 26; Bologna, Italy. [DOI:10.4028/www.scientific.net/KEM.192-195.773]

[20] Xu HHK, Quinn JB. Calcium phosphate cements containing resorbable fibers for short-term reinforcement and macroporosity. Biomaterials. 2002; 23:193-202. [DOI:10.1016/S0142-9612(01)00095-3] [PMID]

[21] Barralet JE, Grover L, Gaunt T, Wright AJ, Gibson IR. Preparation of macroporous calcium phosphate cement tissue engineering scaffold. Biomaterials. 2002; 23:3063-72. [DOI:10.1016/S0142-9612(01)00401-X] [PMID]

[22] Bohner M. Calcium phosphate emulsions: Possible applications. Key Eng Mater. 2001; 192-195:765-8. [DOI:10.4028/www.scientific.net/KEM.192-195.765]

[23] Del Real RP, Wolke JGC, Vallet-Regi M, Jansen JA. A new method to produce macropores in calcium phosphate cements. Biomaterials 2002; 23:3673-80. [DOI:10.1016/S0142-9612(02)00101-1] [PMID]

[24] Almirall A, Larrecq G, Delgado JA, Martinez S, Planell JA, Ginebra MP. Fabrication of low temperature macroporous hydroxyapatite scaffolds by foaming and hydrolysis of an α-TCP paste. Biomaterials. 2004; 25:3671-80. [DOI:10.1016/j.biomaterials.2003.10.066] [PMID]

[25] Sarda S, Nilsson M, Balcells M, Fernandez E. Influence of surfactant molecules as air-entraining agent for bone cement macroporosity. J Biomed Mater Res. 2003; 65A: 215-21. [DOI:10.1002/jbm.a.10458] [PMID]

[26] Hesaraki S, Moztarzadeh F, Sharifi D. Formation of interconnected macropores in apatitic calcium phosphate bone cement with the use of an effervescent additive. J Biomed Mater Res A. 2007; 83(1):80-7. [DOI:10.1002/jbm.a.31196] [PMID]

[27] Hesaraki S, Moztarzadeh F, Solati-Hashjin M. Phase evaluation of an effervescent-added apatitic calcium phosphate bone cement. J Biomed Mater Res Appl Biomater. 2006; 79B:203-9. [DOI:10.1002/jbm.b.30515] [PMID]

[28] Luna LG. Manual of histologic staining method of the armed forces institute of pathology. New York: Mc Graw-Hill Company; 1968. [Link]

[29] Fawcett DW. Bloom and Fawcett: A text book of histology. New York: Chapman and Hall; 1994. [Link]

[30] Jubb KVF, Kennedy P, Palmer. Pathology of domestic animals. Iowa: Academic Press; 1993:1-21. [Link]

[31] Dellmann H.D Eurell J. Textbook of veterinary histology. Baltimore: William & Wilkins; 1998. [Link]

[32] Giavaresi G, Giardino R, Ambrosio L, Battiston G, Gerbasi R, Fini M, Rimondini L, Torricelli P. In vitro biocompatibility of titanium oxide for prosthetic devices nanostructure by low pressure metal organic chemical vapor deposition. Int J Artif Organs. 2003; 26:774-80. [DOI:10.1177/039139880302600811] [PMID]

[33] Kuhne JH, Bartl R, Frisch B, Hammer C, Jansson V, Zimmer M. Bone formation in coralline hydroxyapatite. Effects of pore size studied in rabbits. Acta Orthop Scand. 1994; 65:246-52. [DOI:10.3109/17453679408995448] [PMID]

[34] Ishaug-Riley SL, Crane GM, Gurlek A, Miller MJ, Yasko AW, Yaszemski MJ, et al. Ectopic bone formation by marrow stromal osteoblast transplantation using poly (DL-lactic-co-glycolic acid) foams implanted into the rat mesentery. J Biomed Mater Res. 1997; 36:1-8. [DOI:10.1002/(SICI)1097-4636(199707)36:13.0.CO;2-P]

[35] Lu JX, Flautre B, Anselme K, Hardouin P, Gallur A, Descamps M, et al. Role of interconnections in porous bioceramics on bone recolonization in vitro and in vivo. J Mater Sci Mater Med. 1999; 10:111-20. [DOI:10.1023/A:1008973120918] [PMID]

[36] Rose FR, Cyster LA, Grant DM, Scotchford CA, Howdle SM, Shakesheff KM. In vitro assessment of cell penetration into porous hydroxyapatite scaffolds with a central aligned channel. Biomaterials 2004; 25:5507-14. [DOI:10.1016/j.biomaterials.2004.01.012] [PMID]

[37] Galois L, Mainard D. Bone ingrowth into two porous ceramics with different pore sizes: An experimental study. Acta Orthop Belg. 2004;70:598-603. [PMID]